REPORT DOCUMENTATION PAGE

REPORT DATE	3. REPORT TYPE AND DATES COVERED
	ANNUAL 01 Jan 93 TO 31 Dec 93

SELF-CONSISTEN EFFECTS OF MAGNETOSPHERIC HYDROMAGNETIC WAVES ON RING CURRENT IONS

61102F
F49620-93-1-0101
2311
AS

5. AUTHOR(S)
Dr Mary Hudson

7. PERFORMING ORGANIZATION NAME(S) AND ADDRESS(ES)

Dept of Physics
Dartmouth College
Hanover, NH 03755-3528

8. PERFORMING ORGANIZATION REPORT NUMBER

AFOSR-TR- 94 0113

9. SPONSORING/MONITORING AGENCY NAME(S) AND ADDRESS(ES)

AFOSR/NL
110 DUNCAN AVE SUITE B115
BOLLING AFB DC 20332-0001

Dr Henry Radoski

11. SUPPLEMENTARY NOTES

12a. DISTRIBUTION/AVAILABILITY STATEMENT

Approved for public release;
distribution unlimited

12b. DISTRIBUTION CODE

13. ABSTRACT (Maximum 200 words)

Major progress was made in obtaining an explanation for the rapid formation of new electron and proton radiation belts during the March 30, 1991 geomagnetic storm sudden commencement. Preliminary work on proton acceleration during the same event was reported at the Fall AGU meeting in December. An important feature of the simulation code that has been developed is the ability to post-process data runs after the trajectories of several hundred thousand ions or electrons have been followed through the inbound and outbound propagation time of the wave fields, which is about 100 seconds of real time, As a first step in the development of the three-dimensional MHD fluid-gyrokinetic particle hybrid code, a three-dimensional MHD version of the code in generalized orthogonal coordinates has been developed

14. SUBJECT TERMS			15. NUMBER OF PAGES
			16. PRICE CODE
17. SECURITY CLASSIFICATION OF REPORT (U)	18. SECURITY CLASSIFICATION OF THIS PAGE (U)	19. SECURITY CLASSIFICATION OF ABSTRACT (U)	20. LIMITATION OF ABSTRACT (U)

Annual Technical Report on

AFOSR Grant F49620-93-1-0101

Self-Consistent Effects of Magnetospheric Hydromagnetic Waves on Ring Current Ions

Principal Investigator: Mary K. Hudson
Physics and Astronomy Department
Dartmouth College
Hanover, NH 03755

Reporting Period Covered: January 1 - December 31, 1993

AFOSR Program Manager: Henry R. Radoski
Director of Life and Environmental Sciences
AFOSR/NL
Building 410
Bolling AFB, DC 20332-6558

(a) Objectives

The objective of this research in magnetospheric physics is to advance understanding of the interaction of ring current ions with magnetospheric hydromagnetic waves. In particular, excitation of westward-propagating hydromagnetic waves by a drift-bounce resonance with 100-200 keV ring current protons is being investigated along with the self-consistent nonlinear evolution of the waves and the ring current ion populations (H^+ and O^+). An extension of the ring current particle trajectory tracing code has been used to study the rapid formation of new electron and proton radiation belts, as observed on March 24, 1991.

The methods employed in this research program include (i) numerical solutions of linear gyrokinetic eigenmode equations using existing computer codes, (ii) simulations of the motion of ring current ions in hydromagnetic waves using an existing gyroaveraged Hamiltonian particle code, (iii) development of a 3D dipole geometry magnetohydrodynamic (MHD) code and (iv) coupling of the test-particle and MHD codes to produce a hybrid MHD-gyrokinetic code. The results will provide the first simulation of the excitation and nonlinear evolution of magnetospheric hydromagnetic waves due to ring current ions, and of the self-consistent effect of the waves on the ions. The reduction of storm time ring current fluxes back tc pre-storm levels affects the background magnetic field and the higher-energy radiation belt particle fluxes and spatial distribution. Comparisons with

spacecraft data will be made to test the theoretical predictions and yield new theoretical insights into observed wave properties and associated particle measurements.

(b) Accomplishments

Radiation Belt Results

Major progress was made during this first year in obtaining an explanation for the rapid formation of new electron and proton radiation belts during the March 24, 1991 SSC. A relativistic generalization was implemented of the guiding center test particle code developed by Li et al. (1993a) to follow the trajectories of ring current ions interacting with hydromagnetic waves in the inner magnetosphere. The new code was used with a model for the incoming and outgoing magnetosonic wave imposed on the magnetosphere by the SSC shock impact on March 24, 1991. The acceleration of pre-existing trapped electrons from L = 4 - 9 by the incoming pulse, due to the induction electric field associated with the magnetospheric compression, has been described in the attached reprint (Li et al., 1993b). Remarkable agreement was obtained with the electron drift echoes reported by Blake et al. (1992) at the L = 2.5 nightside position of the CRRES satellite following the SSC, see Fig. 1 of the attached reprint.

Preliminary work on proton acceleration during the same event was reported at Fall AGU (Kotelnikov et al., 1993). The proton source population was taken to be the solar wind shock accelerated protons whose flux was observed to increase in the Aerospace and

other instruments on CRRES preceeding the SSC (Blake, Gussenhoven, private communication; Shea and Smart, 1993). A softer power spectral index ε^{-N} was assumed for the protons (N = 2) than for the electrons (N = 8), consistent with CRRES measurements and those by a Japanese satellite that was on the dayside at the time that the SSC struck the magnetosphere (Blake, private communication). The same model wave field proved to be very efficient at producing proton drift echoes in our simulations with drift periods in agreement with Aerospace omnidirectional data.

An important feature of our simulation code is the ability to post-process runs after we have followed the trajectories of several hundred thousand ions or electrons through the inbound and outbound propagation time of the wave fields (~ 100 s real time). In the post-processing we can vary the assumed initial spectral index choosing a subset of the particle trajectories followed, and incorporate detector response and spacecraft position in order to obtain a best fit of our simulated particle fluxes to those measured by CRRES instruments. This provides us with information about the source population without repeating runs and will allow us to make further comparisons with measurements made by different instruments on CRRES. We particulary look forward to examining the PROTEL data for double peaking in the ion drift echoes evident in the omnidirectional data (Blake et al., 1992). An explanation for this double peaking was suggested in the attached reprint, and our ability to reproduce such features for an instrument with

narrower energy and pitch angle resolution will place additional constraints on our assumed source population and field model.

Ring Current Results

As a first step in the development of the three-dimensional MHD fluid-gyrokinetic particle hybrid code, we have developed a three-dimensional MHD version of the code in generalized orthogonal coordinates. We are currently testing this code. The code has been tested with one, two, and three-dimensional Cartesian coordinates by successfully reproducing the MHD waves and verifying energy conservation. We are now testing the code with curvilinear coordinates, specifically with dipole coordinates. First we tested a two-dimensional version of the code in dipole coordinates successfully with an oscillating magnetic flux bundle isolated from the boundaries of the simulation domain. The results obtained using the dipole coordinates were equivalent to those using the Cartesian coordinate code. Then boundary conditions appropriate for the magnetosphere were introduced. Specifically, a perfectly conducting boundary is implemented for the ionospheric boundary, a constant value or constant gradient boundary is implemented for the radial boundary, and a periodic boundary is assumed for the azimuthal direction. We have reproduced a toroidal field line oscillation at roughly the WKB field line resonance period using the two-dimensional version of the code. Further work is continuing on the boundary conditions and testing of the code in three-dimensional dipole geometry.

Several new results have been obtained from numerical solutions of the linear gyrokinetic eigenmode equations. These results are described in the paper "Anisotropic Alfvén-Ballooning Modes in the Earth's Magnetosphere" by Chan, Xia and Chen, accepted in November 1993 for publication in the Journal of Geophysical Research. In this paper, motivated by spacecraft observations which show that the perpendicular plasma pressure $P_\perp$ is typically larger than the parallel pressure $P_{||}$, we focused on the previously-neglected effects of finite pressure *anisotropy*. Neglecting all kinetic effects and using a self-consistent MHD equilibrium obtained from a multiscale perturbation expansion of an anisotropic Grad-Shafranov equation, we numerically solved the corresponding eigenmode equations using shooting methods. The main results are: (1) The field line eigenfrequency can be significantly lowered by finite pressure effects. (2) The parallel mode structure of the compressional magnetic component can become highly peaked near the magnetic equator due to large perpendicular pressure. (3) For the isotropic case $P_{||} = P_\perp = P$ ballooning instability can occur when the ratio of the plasma pressure to the magnetic pressure, $\beta = P/(B^2/8\pi)$, exceeds a critical value of about 3.5 at the equator. (4) Compared to the isotropic case the critical beta value is lowered by anisotropy. (5) We use a "$\beta - \delta$ stability diagram" to display the regions of instability with respect to the equatorial values of the parameters $\bar{\beta}$ and δ, where $\bar{\beta} = (1/3)(\beta_{||} + 2\beta_\perp)$ is an average beta value and $\delta = 1 - P_{||}/P_\perp$ is a measure of the plasma anisotropy.

The diagram is divided into regions corresponding to the firehose, mirror and ballooning instabilities. (6) It appears that observed values of the plasma pressure are below the critical value for the isotropic ballooning instability but it may be possible to approach a ballooning-mirror instability when $P_{\perp}/P_{||} > 2$.

References

Blake, J.B., W.A. Kolanski, R.W. Fillius and E.G. Mullen, Injection of electrons and protons with energies of tens of MeV into L < 3 on March 24, 1991, Geophys. Res. Lett., 19, 821, 1992.

Li, X., M. Hudson, A. Chan and I. Roth, Loss of ring current O+ ions due to interaction with Pc 5 waves, J. Geophys. Res., 98, 215, 1993a.

Li, X., I Roth, M. Temerin, J.R. Wygant, M.K. Hudson and J.B. Blake, Simulation of the prompt energization and transport of radiation belt particles during the March 24, 1991 SSC, Geophys. Res. Lett., 20, 2423, 1993b.

Shea, M.A. and D.F. Smart, March 1991 Solar-terrestrial phenomena and related technological consequences, Proceedings of 23rd International Cosmic Ray Conference, pg. 739, Calgary, 1993.

(c) Publications

Chan, A.A., X. Mengfen and L. Chen, Anisotropic Alfvén-ballooning modes in the earth's magnetosphere, J. Geophys. Res., in press. 1993.

Li, X., I Roth, M. Temerin, J.R. Wygant, M.K. Hudson and J.B. Blake, Simulation of the prompt energization and transport of radiation belt particles during the March 24, 1991 SSC, Geophys. Res. Lett., 20, 2423, 1993b.

(d) Personnel

PhD researchers involved in the project and receiving support from this grant are:

Dr. Mary K. Hudson

Dr. Anthony A. Chan

Dr. Richard Denton

Dr. Da-Qing Ding

Dr. Xinlin Li

Hudson spent six weeks and Li spent two months at UC Berkeley interacting with Drs. I. Roth, M. Temerin and J. Wygant who are involved with theoretical studies and analysis of data from the CRRES Langmuir Probe Instrument. Additionally, there has been an ongoing exchange of data with Dr. J.B. Blake of the Aerospace Corporation, Principal Investigator for CRRES energetic particle data in the tens-hundred MeV range.

Dartmouth PhD Graduate student Alexei Kotelnikov receives support from this grant, for his thesis work on proton acceleration in the March 24, 1991 event. Jerry Goldstein and Marc Lessard, PhD graduate students, receive support under the related AASERT grant for work on hydromagnetic wave data analysis in the ring current region and substorm injection into the ring current, respectively.

(e) Interactions

Abstracts

Chan, A.A. and L. Chen, Stability of anisotropic Alfvén - ballooning modes in the Earth's magnetosphere, EOS Trans Am. Geophy. Union, 74 (Fall Meeting), 506, 1993.

Ding, D.Q., M.K. Hudson and R.E. Denton, Modelling of ring current ion interaction with magnetospheric hydromagnetic waves: prelminary results, EOS Trans. Am. Geophys. Union, 74 (Fall Meeting), 504, 1993.

Kotelnikov, A.D., M.K. Hudson, X. Li, I. Roth, M. Temerin, J. Wygant and J.B. Blake, Numerical simulation of radiation belt ion acceleration in the March 24, 1991 SSC, EOS Trans. Am. Geophys. Union, 74 (Fall Meeting), 504, 1993.

Li, X., I. Roth, M. Temerin, J. Wygant, M.K. Hudson and J.B. Blake, EOS Trans. Am. Geophys. Union, 74 (Spring Meeting), 264, 1993.

Temerin, M., I. Roth, J. Wygant, X. Li, M.K. Hudson and J.B. Blake, Further results from the simulation of the March 24, 1991 drift echo event Trans. Am. Geophys. Union, 74 (Fall Meeting), 517, 1993.

(i) Seminars

Dartmouth (Chan, Denton, Hudson, Li)
Progress on ring current and radiation belt code development

X. Li (Same title as GRL)
UC Berkeley
Dartmouth
National Research Council of Canada, Herzberg Institute, Ottawa
Philips Laboratory, Bedford, MA

(ii) Consultative and advisory functions

Denton visited Phillips laboratory in June and presented a progress report on ring current code development and radiation belt studies. Li visited Philips Laboratory in December and consulted with Mullen and Gussenhoven on CRRES low energy electron and proton data. Hudson plans a visit in January to discuss application of our model to CRRES PROTEL data. Hudson has been in frequent contact with Blake of The Aerospace Corporation on more energetic particle data from CRRES, and arranged a working meeting at the Fall AGU of all parties involved with the electron and proton drift echo studies (GRL co-authors).

GEOPHYSICAL RESEARCH LETTERS, VOL. 20, NO. 22, PAGES 2423-2426, NOVEMBER 19, 1993

SIMULATION OF THE PROMPT ENERGIZATION AND TRANSPORT OF RADIATION BELT PARTICLES DURING THE MARCH 24, 1991 SSC

Xinlin Li[1], I. Roth[2], M. Temerin[2], J. R. Wygant[2], M. K. Hudson[1], J. B. Blake[3]

Abstract. We model the rapid ($\sim$ 1 min) formation of a new electron radiation belt at $L \simeq 2.5$ that resulted from the Storm Sudden Commencement (SSC) of March 24, 1991 as observed by the CRRES satellite. Guided by the observed electric and magnetic fields, we represent the time-dependent magnetospheric electric field during the SSC by an asymmetric bipolar pulse that is associated with the compression and relaxation of the Earth's magnetic field. We follow the electrons using a relativistic guiding center code. The test-particle simulations show that electrons with energies of a few MeV at $L > 6$ were energized up to 40 MeV and transported to $L \simeq 2.5$ during a fraction of their drift period. The energization process conserves the first adiabatic invariant and is enhanced due to resonance of the electron drift motion with the time-varying electric field. Our simulation results, with an initial W^{-8} energy flux spectra, reproduce the observed electron drift echoes and show that the interplanetary shock impacted the magnetosphere between 1500 and 1800 MLT.

Introduction

At 3:41 UT on March 24, 1991 an almost instantaneous formation of a new electron radiation belt was observed by the CRRES satellite which was fortuitously situated at a distance of 2.55 R_E near the equatorial plane at a local time of 0300 MLT [Vampola and Korth, 1992; Blake et al., 1992]. The creation of the radiation belt was accompanied by an electron and ion drift-echo event from which Blake et al. [1992] deduced that the injected electrons were at energies predominately above 15 MeV with an energy spectral index of -6. This radiation belt lasted beyond the end of the CRRES mission six months later. The event was apparently initiated by an interplanetary shock that compressed the magnetosphere inside geostationary orbit. The shock was also detected by Ulysses at a distance of 2.5 AU and by interplanetary scintillation measurements from which it was inferred that the shock approached the Earth in the afternoon sector [Woan and Hewish, private communication].

The measured electric field was seen as a bipolar pulse, predominantly in the azimuthal direction, with a peak-to-peak magnitude of 80 mV/m and in the magnetic field as an 140 nT monopolar pulse with a duration of 120 s [Wygant et al., 1993], consistent with ground magnetometer measurements of a narrow impulse [Yumoto and Shiokawa, private communication]. Wygant et al. [1993] argue, based on previous measurements of the local time dependence of field perturbations associated with SSCs [Schmidt and Pederson, 1987], that the field enhancements were much larger on the dayside.

The observed creation of this electron belt is an unique event in space physics which raises new questions about the formation of radiation belts in general and about the specific mechanisms that produced this electron belt in particular [Blake et al., 1992]. In this Letter we present results from a test-particle simulation of the interaction of energetic electrons with electric and magnetic fields during the SSC. The left column of Figure 1 shows the electron data from Blake et al. [1992] together with the electric and magnetic fields from Wygant et al. [1993]. Questions that these data present and that we address are: (a) How did the > 6 MeV electron flux rise in 10 s at $L = 2.5$ by four orders of magnitude? (b) What is the source of the electrons seen at $L \simeq 2.5$? (c) What causes the oscillations in the subsequent electron flux?

Model

We model the unperturbed magnetosphere as a dipole magnetic field $\mathbf{B}_E$. The interaction of the interplanetary shock with the geomagnetic field compresses the magnetosphere. The compression is modelled as a time dependent Gaussian pulse with a purely azimuthal electric field component that propagates radially inward at a constant velocity, decreases away from the impact point, and is partially reflected near the surface of the Earth. The modelled shock encounters the magnetosphere first at longitude ϕ_0 and subsequently at other longitudes. Explicitly, in the usual spherical coordinates (r, θ, ϕ), where $r > R_E$ is measured from the center of the Earth, $\phi = 0°$ at noon local time, positive eastward, $\theta = 0°$ at the north pole, the electric field is given by

$$\mathbf{E}_w = -\hat{e}_\phi E_0 \Big(1 + c_1 \cos(\phi - \phi_0)\Big) \Big[\exp(-\xi^2) - c_2 \exp(-\eta^2)\Big], \quad (1)$$

where the terms in the square brackets are associated with the compression and relaxation of the magnetosphere. In (1) $\xi = [r + v_0(t - t_{ph})]/d$, $\eta = [r - v_0(t - t_{ph} + t_d)]/d$, v_0 is the pulse propagation speed, and d is the width of the pulse; $c_1 (> 0)$ describes the local time dependence of the electric field amplitude, which is largest at ϕ_0; $t_{ph} = t_i + (c_3 R_E/v_0)[1 - \cos(\phi - \phi_0)]$ represents the delay of the pulse from ϕ_0 to other local times; c_3 determines the magnitude of the delay; c_2 determines the partial reflection of the pulse; $t_d = 2.06 R_E/v_0$ indicates that the reflection occurs at $r = 1.03 R_E$; and t_i determines the location of the pulse at the start of the simulation. In this Letter we present results with E_0= 240 mV/m, $c_1 = 0.8, c_2 = 0.8, c_3 = 8.0$, v_0= 2000 km/s, t_i= 80 s, $\phi_0 = 45°$ and d= 30,000 km. At $t = 0$ the pulse is at about $25 R_E$.

The perturbed magnetic field $\mathbf{B}_w$ is obtained from Faraday's law and satisfies $\nabla \cdot (\mathbf{B}_E + \mathbf{B}_w)$=0 and $\mathbf{E}_w \cdot (\mathbf{B}_E + \mathbf{B}_w)$=0. The model thus describes the propagation of a magnetosonic pulse through the magnetosphere ignoring the variable pulse velocity due to changes in density, temperature and magnetic field. The bottom right panels of Figure 1 show the electric and magnetic field given by the model at $L = 2.5$ and at $\phi - \phi_0 = 180°$ (0300 MLT). At other local times the form of the pulse is the same but its amplitude is larger. At larger L values the pulse is broader and somewhat larger since the incoming and reflected pulses are further separated and there is less destructive interference between them. The model parameters were chosen to approximate the data on the basis of physical reasoning and some limited experimentation. We

[1]Dartmouth College, Hanover, New Hampshire
[2]University of California, Berkeley, California
[3]The Aerospace Corporation, Los Angeles, California

Paper number 93GL02701
0094-8534/93/93GL-02701$03.00

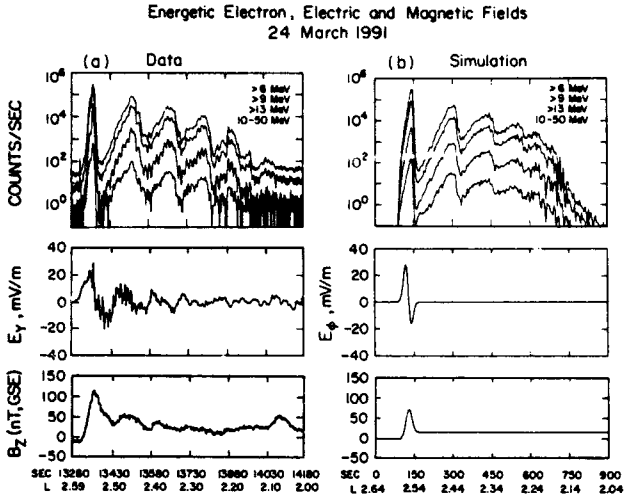

Fig.1. a) Data from the CRRES satellite at the time of the March 24, 1991 SSC . op panel shows count rates as a function of time from four energetic electron channels measuring integral counts above a threshold energy indicated, and also over 10-50 MeV [Blake et al., 1992]. Middle and bottom panels show the measured electric field E_y in a co-rotational frame and the B_z magnetic field component with a model magnetic field subtracted, in GSE coordinates over the same time interval [Wygant et al., 1993]. b) Simulated results in the same format as (a) measured at a spatial location corresponding to the trajectory of the CRRES satellite, including the Aerospace detector responses in the top panel. Time is measured from t =0 as determined by (1).

varied the velocity, v_0, between 750 and 2000 km/s, the field amplitude, E_0, between 120 and 240 mV/m, and used impact angles of 0°, 45°, and 90°. We found that the chosen parameters approximate the electron data well.

We follow the particles using a relativistic guiding center approximation with $v_{\|} = 0, E_r = E_\theta = 0$ [Northrop, 1963]

$$\dot{W} = q\dot{\mathbf{R}}_\perp \cdot \mathbf{E}_w + \frac{M_r}{\gamma}\frac{\partial B}{\partial t}, \qquad (2)$$

$$\dot{\mathbf{R}}_\perp = \frac{\hat{e}_1}{B} \times (-c\mathbf{E}_w + \frac{M_r c}{\gamma e} \nabla B), \qquad (3)$$

where $\dot{\mathbf{R}}_\perp$ describes the guiding center motion perpendicular to the instantaneous magnetic field $\mathbf{B} = \mathbf{B}_E + \mathbf{B}_w$, $\hat{e}_1 = \mathbf{B}/B$ is a unit vector along $\mathbf{B}$, $\gamma = (W + m_0c^2)/m_0c^2$ is the relativistic energy factor, W is the particle's kinetic energy, $M_r = p_\perp^2/2m_0B$ is the relativistic adiabatic invariant and $p_\perp$ is the particle's perpendicular momentum.

In the simulation we follow 336,720 electrons as they drift in the combined fields of the Earth's dipole and the modelled pulse field, recording their energy, arrival time, radial distance, and initial conditions as they pass various local times. We model the relativistic population of electrons before the event by distributing test-particle electrons in the equatorial plane at distances from L=3 to L=9 in increments of 0.1 R_E, in azimuth every 3°, and at energies between 1 and 9 MeV in increments of 5%. We restrict ourselves to 90° pitch angles following the indication from the particle detectors of an equatorially trapped electron population [Blake et al., 1992]. In the post-processing stage each electron is given a weight which depends on the assumed initial distribution in energy (power law) and in L. The initial distribution in L is modelled by a parabola $G(L) = 1-(L-L_0)^2/a_0^2$. Here, we have taken the power law index -8, with the variation in L determined by L_0 = 10 and a_0 = 7.5. Thus, given an initial electron distribution, we obtain electron fluxes and distributions at any location and compare the simulation results with the CRRES observations, incorporating the energy response of the Aerospace energetic electron detectors [Blake et al., 1992].

Results and Discussion

The right column of Figure 1 shows the simulated electron flux and fields near the CRRES position at 0300 MLT and L = 2.5. Each point in the upper panel shows the flux over a three second interval with the corresponding detector characteristics folded in and integrated over L values ± 0.1 R_E around the CRRES position. The simulated L values were chosen to match those of the satellite at the time of the first pulse and to follow the orbit of CRRES. The agreement between the simulation and the data is quite remarkable. This agreement includes the relative amplitudes and periods of the first three drift echoes. Repeated pulses reflect the drift period, the sawtooth shape reflects the fact that the more energetic electrons which have a lower flux reach the detector sooner, and the abrupt cutoff is due to the low flux of lower energy electrons.

Since higher energy electrons drift faster, the magnetosphere acts as a giant energy spectrometer. The temporal slope of the flux at a specific location depends on the velocity dispersion. From the slope of the second drift-echo peak, Blake et al. [1992] were able to deduce that the energy spectrum of the injected electrons on CRRES peaked at about 15 MeV, extended up to 50 MeV, and had a power law spectrum of W^{-6}. In the simulations we found that an initial spectrum of W^{-8} between 1 MeV and 9 MeV produced the best agreement with the data.

The magnetospheric source of the drift echo electrons can be determined by comparing the measured electron spectrum in the outer magnetosphere with the measured flux at L=2.5, assuming that the phase space density of electrons is conserved. This implies that the flux varies as $j \propto L^{-3}$ [Lyons and Williams, 1984]. Thus the measured flux at L=2.5 at 14 MeV requires an initial flux four times less at L=4 at 6.9 MeV or 27 times less at L=7.5 at 2.7 MeV. (We note that conservation of the first adiabatic invariant for 90° pitch angle relativistic electrons implies that the electron energy $W \propto B^{1/2} \propto L^{-3/2}$ since $W \sim pc$.) CRRES observed the background electron flux prior to the drift-echo event during the inbound part of its orbit from L=6.8. The CRRES Cerenkov counters provide only an upper limit due to contamination from penetrating solar protons that preceded the shock by about a day and populated the magnetosphere beyond $L > 4$. This upper limit shows that there was insufficient electron flux at $L < 5$. Between L=5 and L=6.8 the Lockheed spectrometer measured electrons up to 5 MeV, but was subject to the same contamination above 2 MeV. Extrapolating the measured flux below 2 MeV [Nightingale, private communication] shows that there was sufficient flux beyond L=6. However, the extrapolation should be interpreted as an upper limit since it uses the spectral index -2.7 to -4 measured below 2 MeV, rather than the spectral index -6 to -8 inferred from the data and the simulation at higher energies. Thus we conclude that the source of the drift-echo electrons was beyond L=6, consistent with our simulation in which most of the flux is from $7 < L < 9$.

The local time of the shock impact determines the width of the first drift-echo peak. In Figure 1 the shock impacted at 1500 MLT. When we choose 1200 MLT, the first peak in the electron flux was noticeably wider than in the data due to increased energy dispersion of the electrons as they drift east from a larger distance. When we choose 1800 MLT, the first peak was noticeably narrower due to decreased dispersion. For 1500 MLT, as shown in Figure 1, the first

peak is just slightly wider than in the data. Thus our simulations are in agreement with Blake et al. [1992], who deduced from the ion and electron data that the shock impacted in the afternoon sector at about 1600 MLT.

Figure 2 shows the electron energy spectra at several L values integrated over a drift period. A remarkable aspect of the spectra is the sharp rise in the flux at higher energies. As the shock-induced distortion of the magnetosphere propagates away from the point of initial impact, higher energy electrons, which gradient-drift faster, stay in phase longer with the perturbation and thus are convected in further. However, as seen in our simulation, the most energetic electrons can also outrun the optimum drift speed and thus are not convected as far inward. From Figure 2 one sees that the low energy cutoff of the electron flux decreases with increasing L. At the lowest energies there is again a rise in the electron flux because electrons originally at low L values ($3 < L < 4$) $\mathbf{E} \times \mathbf{B}$ drift inward without optimally matching the drift-resonance condition. These electrons have, however, a small phase-space density at higher energies because they have gained relatively little energy in moving inwards and because of the initial W^{-8} energy spectrum. Conversely the largest flux is contributed by electrons from the largest L values in the simulation. Most of the simulated flux at $L = 2.5$ is due to electrons originally at L values between 7 and 9.

Low energy electrons are affected mainly by the $\mathbf{E} \times \mathbf{B}$ drift and their motion is indicative of the relative motion of the magnetospheric plasma and of the magnetopause. At 1500 MLT, the impact location of the shock, zero energy electrons from L =8.5 were convected inward to $L = 3.84$ and then back to $L = 5.51$ by the reflected pulse; directly on the opposite side of the magnetosphere from the shock the corresponding L values were 6.44 and 7.83. However, electrons with the optimum energy and azimuth at L =8.5 were convected to $L = 2.26$. An electron starting with an energy of 2.53 MeV at L=8.5 reached a final L value of 2.27 and a final energy of 21 MeV. An electron with an initial energy of 8.99 MeV and an initial position of $L = 9$ acquired the most energy. Its final energy was 49.3 MeV at L=2.99. Electrons starting at lower L values with the optimum initial local time and energy will always penetrate to lower L values than electrons starting at larger L values with the same magnetic moment; however, no electrons in our simulations penetrate below $L = 2$. We conclude that energetic electrons drifting in phase with the wave-field perturbation can move to much lower L values than low energy electrons which track the magnetosphere distortion. Figure 3 shows the time evolution of a ring of electrons initially at $L = 7$ with an energy of 4 MeV. This figure illustrates the distortion of the initial energetic electron distribution produced by the shock. Rings at other L values with the same magnetic moment are nested within or outside the deformed ring in a similar manner.

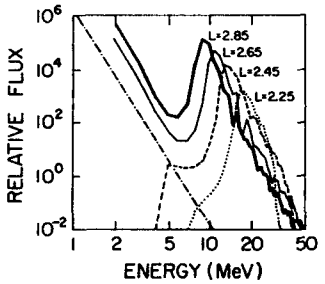

Fig. 2. Simulated electron energy spectra at L= 2.25, 2.45, 2.65 and 2.85 $\pm\Delta L = 0.1$ in each case and averaged over a drift period. Vertical axis is logarithmic in counts vs. energy in MeV, and spectra are binned in 1 MeV increments and plotted at the upper limit of each bin. Input simulation spectrum at $L = 8.5$ is plotted as the dot-dashed power law on the left.

The electron energy gain is very sensitive to the local time. Those electrons which stay in phase with the reflected pulse longer than with the incoming pulse, or encounter the incoming pulse on the night side where it is relatively weak, may lose energy. Figure 4 shows the trajectories of three electrons starting at L =8.5. Two of the electrons reach a final L value of 2.5 while the third escapes the simulation region ($L > 12$). Electron A reaches an energy of 37.3 MeV starting from an initial energy of 5.52 MeV while electron B reaches a final energy of 13.1 MeV starting with an energy of 1.71 MeV. Electron C starting with an energy of 5.52 MeV escapes the magnetosphere by interacting more strongly with the reflected pulse than with the incoming pulse. Note that during part of its trajectory electron A moves radially inward. This is because the magnetic field of the inward propagating pulse cancels the normal inward gradient of the dipole magnetic field and thus for a while there is little gradient drift. During this phase the electron gains its energy only from the second term in (2). Electrons like B, however, contribute much more to the flux at L =2.5 since the assumed initial energy distribution (W^{-8}) implies that there are many more such lower energy electrons.

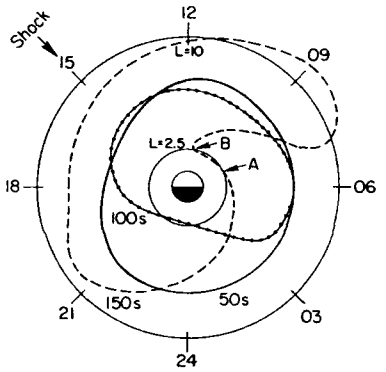

Fig. 3. Time evolution of an electron ring in $L - \phi$ space, at 50 s intervals from the beginning of the simulation. The electrons were placed initially at $L = 7$ with an energy of 4 MeV and longitudinal spacing of 0.5°.

Electrons injected at a given point at time t_0 will arrive at the detector at time $t = t_0 + \delta/v_D$ where δ is the distance along the drift path and v_D is the drift velocity which, for relativistic electrons, is closely proportional to their energy. This implies that $1/v_D = (1/\delta)(t - t_0)$. Thus the points on a plot of $1/v_D$ versus t should be aligned along a straight line with a slope of $1/\delta$ and an intercept of t_0 if all the electrons were injected at the same location and time. Figure 5 is such a plot for the first three drift echoes for all the electrons that passed 0300 MLT between $2.46 < L < 2.54$. This figure can also be interpreted as an energy-time plot of the electrons with the energy given on the right-hand side. Since all electrons are plotted as dots there is no weighting involved. To a good approximation, the electrons do in fact fall on a line from which it is possible to determine, following the reasoning above, that they were injected at the approximate time $t_0 = 83$ s and at a position corresponding to 1930 MLT. This, however, does not correspond to where the SSC impacted the magnetosphere in the model and as inferred from data. Instead, the simulated perturbation was centered at 1500 MLT and the electrons were accelerated over finite local times and radial distances. The straight dashed line in Figure 5 corresponds to the injection of all electrons at 1500 MLT and $L = 2.5$.

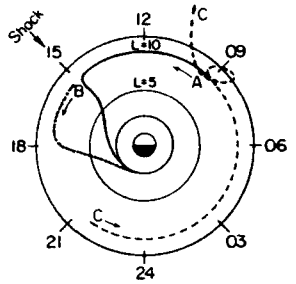

Fig. 4. Simulated trajectories of three equatorially mirroring electrons starting at L=8.5. Electrons A, B, and C start at 0900, 1500, and 2100 MLT, respectively.

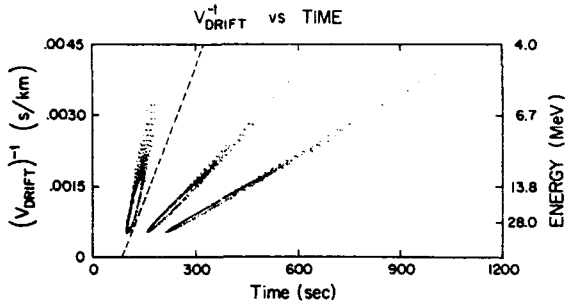

Fig. 5. Plot of $1/v_D$ vs. t for all particles in the simulation which intersect $L = 2.5 \pm 0.04$ at 0300 MLT. The three sets of points correspond to the first three drift echoes. The dashed line is the loci of points expected if all the particles were injected simultaneously at 1500 MLT at L=2.5.

In contrast to the local injection scenario, the lower energy electrons are accelerated closer to the spacecraft where the wave field is weaker while higher energy electrons are accelerated farther from the spacecraft where the wave field is stronger. Injections commonly seen at geosynchronous orbit often have energy dispersion from which injection distances can be calculated [Belian et al.,1978]. Based on our results, one should be very cautious in inferring the magnetic local time of injection or energization.

Another feature of Figures 3 and 5 is the hole in the electron flux at energies between 12 MeV and 30 MeV. Had these electrons been measured by a detector with narrow energy resolution, this gap would have appeared as a double peak in the electron flux vs. time at these energies. Double peaks were observed in the ion flux during this event [Blake et al., 1992] and are commonly seen in ion drift-echo events at geosynchronous orbit [Belian et al.,1984]. The hole maps to the space between A and B in Figure 3. Due to the lack of electrons at $L > 9$ in the model, empty phase space extends inside $L = 2.5$.

Conclusions

The most important conclusion of our simulation is that the electron injection and drift-echo event of March 24, 1991 can be understood as a consequence of a simple model of the electric and magnetic field perturbations in the magnetosphere initiated by the interaction of an interplanetary shock with the magnetosphere. While our model of the electric and magnetic fields is simplified, and other models may produce similar results, it incorporates enough realistic features to model this electron drift-echo event. As a consequence we confirm that the shock impacted the magnetosphere in the afternoon sector, that it compressed the magnetosphere inside geosynchronous orbit, probably to about 4 R_E, and that the electrons were energized to about 50 MeV in less than 100 s. In addition we show that, although the injection time and location is well-defined by the energy dispersion of the simulated electrons, this location does not correspond to the actual region where the electron energization took place. Future work will include the effects of a variable pulse speed due to the interaction with the plasmasphere, off-equatorial electrons and the acceleration of ions, including the double peak effect noted here.

Acknowledgments. The authors are indebted to A. A. Chan for useful preliminary discussion, H. Voss and R. Nightingale for useful discussion of the Lockheed energetic electron data, and K. Yumoto and K. Shiokawa of the Solar-Terrestrial Environment Lab., Nagoya University for providing measurements by the 210 Degree MM Magnetic Observation Group. Work at The Aerospace Corporation was supported by the Air Force under contract F04701-88-C-0089; at Dartmouth and UC Berkeley by NASA Grants NAG 5-1098, NAGW-1626, and AFOSR grant F49620-93-1-0101 and Air Force contracts F19628-87-K0016 and F19628-92-K0009. Computations were performed on the SDSC Cray and NCSA Cray.

References

Belian, R. D., D. N. Baker, P. R. Higbie, and E. W. Hones, Jr., High-Resolution Energetic Particle Measurements at 6.6 R_E, 2, High-Energy Proton Drift Echoes, *J. Geophys. Res.*, *83*, 4857, 1978.

Belian, R. D., D. N. Baker, E. W. Hones, and P. R. Higbie, High-energy proton drift echoes: multiple peak structure, *J. Geophys. Res.*, *89*, 9101, 1984.

Blake J. B., W. A. Kolasinski, R. W. Fillius, and E. G. Mullen, Injection of electrons and protons with energies of tens of MeV into $L < 3$ on March 24, 1991, *Geophys. Res. Lett.*, *19*, 821, 1992.

Lyons, L. R. and D. J. Williams, Quantitative aspects of magnetospheric physics, p.201, D. Reidel, Boston, 1984.

Northrop, T. G., The adiabatic motion of charged particles. Interscience Publishers, New York, 1963.

Schmidt, R. and A. Pederson, Signature of storm sudden commencements in the electric field measured at geostationary orbit (GEOS-2), *Physica Scripta*, 491, 1987.

Vampola, A. K., A. Korth, Electron drift echoes in the inner magnetosphere, *Geophys. Res. Lett.*, *19*, 625, 1993.

Wilken B., C.K.Goertz, D.N.Baker P.R.Higbie and T.A.Fritz, The SSC on July 29,1977 and its propagation within the magnetosphere, *J. Geophys. Res. 87*, 5901, 1982

Wygant, J. R., F. Mozer, J. B. Blake, N. Maynard, H. Singer and M. Smiddy, Large amplitude electric and magnetic field signatures in the inner magnetosphere during injection of 15 Mev electron drift echoes, *Geophys. Res. Lett.*, in press, 1993.

M. K. Hudson and X. Li, Department of Physics and Astronomy, Dartmouth College, Hanover, NH 03755-3528.

I. Roth, M. Temerin and J. R. Wygant, Space Science Laboratory, University of California, Berkeley, CA 94720.

J. B. Blake, The Aerospace Corporation, Los Angeles; CA 90009-2957.

(Received August 5, 1993;
accepted September 13, 1993.)